Influence of an Ethylene-Octene Copolymer and of Pollutants in PP/EPR Blends

Nizar Mnif,[1,2] Valérie Massardier-Nageotte,[1] Mohamed Jaziri[2]

[1]*Laboratoire des Matériaux Macromoléculaires, Institut National des Sciences Appliquées de Lyon, Unité Mixte de Recherche Centre National de la Recherche Scientifique (INSA Lyon)-UMR/CNRS 5627, 69621 Villeurbanne Cedex, France*
[2]*Laboratoire Eau/Energie/Environnement, Ecole Nationale des Ingénieurs de Sfax (ENIS), Rte Soukra 3038, Sfax, Tunisie*

Received 12 January 2006; accepted 3 June 2006
DOI 10.1002/app.25946
Published online 8 March 2007 in Wiley InterScience (www.interscience.wiley.com).

ABSTRACT: The objective of this work was to study the effectiveness of commercial compatibilizers (E-EA-MAH copolymer) on the morphology of blends of polypropylene/ethylene polypropylene rubber (PP/EPR) (78/22) and metallocenic ethylene-octene copolymer (EOC) polluted by (poly (vinyl chloride) (PVC) and by an oil for engine. Blends of various compositions (with and without compatibilizer or pollutant), were prepared using a corotating twin-screw extruder. In both cases, the analyses of blend morphologies highlighted the poor adherence between the two phases in the uncompatibilized blends. Compatibilized polluted blends display better adherence between phases. Dynamic mechanical thermal analysis and differential scanning calorimetry show that the compatibilizer improves the adhesion between both phases and enables stress transfer at the interface. © 2007 Wiley Periodicals, Inc. J Appl Polym Sci 104: 3220–3227, 2007

Key words: polypropylene; ethylene-octene copolymer; blends; morphology; rheological properties; thermal properties; recycling

INTRODUCTION

Most of the time, the recycling of mixed plastic wastes induces complex sorting to separate each component. Nevertheless, not all the polymers can be separated because of the use of polymer blends and stuck parts. Thus, the recycling of polymer blends is a new challenge for environmental protection.

With an annual production of more than 250,000 tons in Europe, polypropylene is one of the most widely used polymers. Polypropylene is present in automobiles, household appliances, etc. To overcome its high flammability, tendency to brittleness at temperatures below its glass transition temperature and low stiffness, polypropylene can be modified with fillers and elastomers such as ethylene propylene rubber (EPR) and ethylene propylene diene monomer (EPDM).

An emerging catalytic system, termed single-site catalyst (metallocene type), allows polymer producers to sell well-defined molecules called ''plastomers'' with lateral alkyl functions[1,2] that can be used as elastomers. One family of these new polymers produced by Dow Chemicals, called Engage polyolefin elastomers or ''plastomers,'' was used in this study. These elastomers, containing oct-1-ene as comonomer, have distinctive properties due to hexyl chain branching. These materials are aimed for competing with thermoplastic olefin impact modifiers, like EPDM.[3,4]

Polypropylene (PP)/elastomer blends[5–8] have been extensively studied with the objective of improving their recycling with compatibilizers but the effect of pollutants has not been studied and there are only a very few publications in this field.[9] Although it can be assumed that some pollutants are detrimental for the properties of recycled materials, others, such as oils, may be expected to improve some mechanical properties (Charpy impact for example).[10]

In the present work, the objective was to elaborate model blends to better understand the behavior of the materials that could result from the sorting and recovery of various polypropylene formulations containing either EPR or EOC and other pollutants. Thus, the morphological, thermal, and rheological properties of (PP/EPR) formulations blended with commercial ethylene-octene copolymer (EOC) and pollutants were studied.

Poly(vinyl chloride) (PVC) and an oil for engine have been chosen as pollutants.

EXPERIMENTAL

Materials

The materials used in this work, (PP/EPR), EOC, and E-EA-MAH, are all commercially available grades.

Correspondence to: V. Massardier-Nageotte (valerie.massardier@insa-lyon.fr).

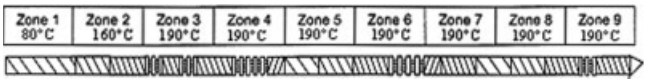

Figure 1 Twin-screw extruder; screw and temperature profile.

(PP/EPR) (78/22) (PP108MF97), supplied by Sabic, is made of a polypropylene matrix (78 wt %) containing an EPR (about 50% of ethylene) (22 wt %) phase (specific gravity, 0.905 g/cm^3; melt flow index (MFI), 10 g/10 min under 2.16 kg at 230°C).

Ethylene-octene copolymer (EOC) (Engage 8842) was supplied by Dupond Dow; specific gravity, 0.857 g/cm^3; MFI, 1.0 dg/min).

E-EA-MAH (Lotader 3210), supplied by ATOFINA, is a random terpolymer of ethylene (E), acrylic ester (AE), and maleic anhydride (MAH) (specific gravity, 0.94 g/cm^3; melt flow index (MFI), 5 g/10 min under 2.16 kg at 190°C).

Preparation of blends, morphologies, rheological, and thermal properties

Homopolymers with and without a compatibilizer were premixed as pellets to the required proportions prior to processing in a corotating twin-screw extruder (Clextral BC 21: D = 25 mm, L/D = 36). The screw and temperature profiles used in this study are given in Figure 1. The rotational speed of twin-extruder is 200 revolutions per minute. Table I illustrates the composition of the blends. First, pellets of (PP/EPR)/EOC and (PP/EPR)/EOC/E-EA-MAH were elaborated with the twin-screw extruder. Then, those (PP/EPR)/EOC and (PP/EPR)/EOC/E-EA-MAH pellets were extruded again, in the same conditions, with either oil or PVC.

The morphologies were analyzed on 4-mm-thick specimens prepared by injection molding with a press Battenfeld Unilog B2; 350 Plus. The temperature ranged from 190 to 200°C for the (PP/EPR)/EOC (80)/20 blends. The morphologies of the blends were observed with a scanning electron microscope (SEM Philips XL 30). Samples were fractured in liquid nitrogen. The fractured surfaces of the specimens were observed after gold coating under an accelerating voltage of 30 kV.

DSC analyses and dynamic rheological properties were analyzed on 1-mm-thick films prepared by compression molding. Blends were placed in a preheated table press and pressed into the shape of plates under 30 bars at 180°C for the (PP/EPR)/EOC (80)/20 blends. After 10 min, the plates were transferred into a second press cooled with water to control the cooling ramp (36°C/min).

The thermal analyses were performed under argon using a differential scanning calorimeter DSC 30 of Mettler-Toledo SA. Standard aluminum pans were used. Samples (10–20 mg) were weighted directly in the pan and an empty pan was used as a reference. Temperature calibration was performed using indium. Experiments were carried out between −100 and 200°C; heating rates were both set to 10°C/min.

The measurements of the rheological properties were made using a Rheometrics dynamic analyzer (RDA 700) with sample specimens having the following dimensions: length 20 mm, width 6 mm, and thickness ~ 1.5 mm. The loss tangent (tan δ) was measured between −100 and 200°C at a constant frequency of 6.28 Hz and a heating rate of 2°C/min.

RESULTS AND DISCUSSION

Morphologies of binary, compatibilized, and polluted blends

(PP/EPR)/EOC blends

It has been reported that the rheological properties of elastomer/plastic blends can be related to the mode and state of dispersion of the minor component.[11] Martuscelli and coworkers[12] showed that, for (PP/EPR) systems, $\eta_{0(blend)}$ and $\tau_{0(blend)}$ values decrease with increasing dispersion coarseness of the minor component.

The analysis of PP/EPR 78/22, by SEM [Fig. 2(a)], displays a nodular morphology where the EPR phase is dispersed as spherical particles. The talc plates are well distributed; their surface is clean and free of any polymer. This indicates a relatively weak adhesion between the mineral and the polymer. On the other hand, we observe the empty cavities that

TABLE I
Composition of the Blends

Blends	(PP/EPR) (78/22) (%)	EOC (%)	E-EA-MAH (%)	Oil (%)	PVC (%)
(PP/EPR)/EOC	80	20	0	0	0
(PP/EPR)/EOC/E-EA-MAH	80	16	4	0	0
(PP/EPR)/EOC/oil	76	19	0	5	0
(PP/EPR)/EOC/PVC	76	19	0	0	5
(PP/EPR)/EOC/E-EA-MAH/oil	76	15.2	3.8	5	0
(PP/EPR)/EOC/E-EA-MAH/PVC	76	15.2	3.8	0	5

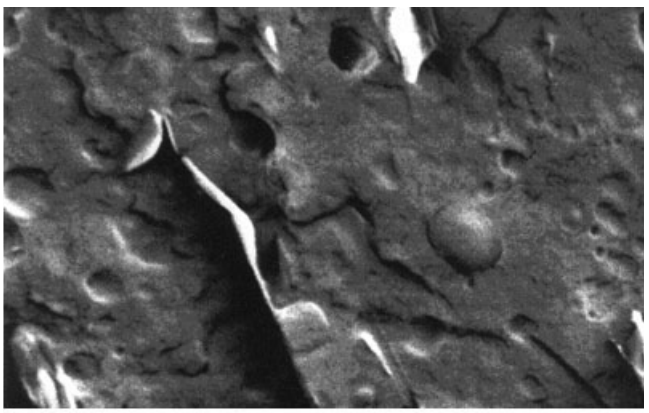

(a)

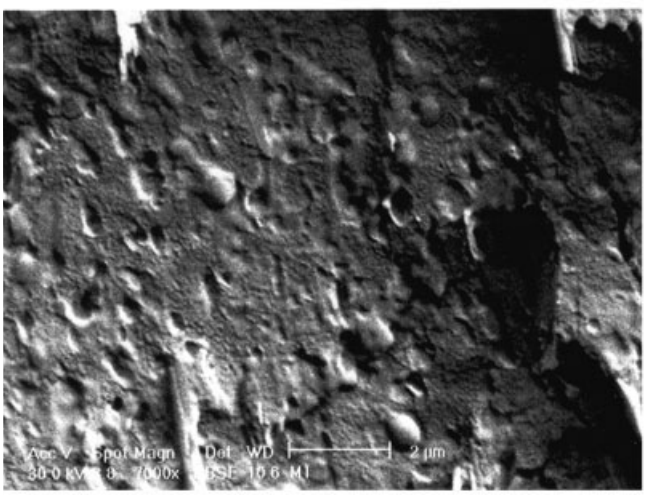

(b)

Figure 2 Morphologies of (a) (PP/EPR) (78/22) and (b) (PP/EPR)/EOC (80)/20 blends elaborated with the twin-screw extruder.

correspond to the deformed particles of the EPR phase. Scanning electron micrographs of fracture surfaces in a (80)/20 (PP/EPR)/EOC (80)/20 blend [Fig. 2(b)] represent a nodular morphology in the same way; the EOC phase is dispersed in the form of aggregated particles of uncertain shape (1–2 µm). The adhesion between PP/EPR 78/22 and EOC phases is assigned to the interactions between the ethylene sequences of both phases.

Effect of the compatibilizer in the (PP/EPR)/EOC (80)/20 blend

Figure 3(a,b) are scanning electron micrographs of the fracture surfaces of (PP/EPR)/EOC (80)/20 and (PP/EPR)/EOC/E-EA-MAH (80)/16/4 systems. The evolution of the morphological structure of the (PP/EPR)/EOC/E-EA-MAH blend is assigned to the nature of the compatibilizer used. Thus, the ethylene sequences of the E-EA-MAH copolymer are going to contribute to the improvement of the partial miscibility of (PP/EPR) (78/22) and EOC phases, due to interactions between the ethylene sequences of the various copolymers present in the blend. The E-EA-MAH copolymer should be preferentially localized at the interface of (PP/EPR) 78/22 and EOC phases generating an improved adherence, which is going to assure a better cohesion of the whole material.

Effect of pollutants in the (PP/EPR)/EOC (80)/20 blend

Figure 4(b) displays the morphology of the fractured surface of the (PP/EPR)/EOC/oil (76)/19/5 blend. The SEM analyses revealed a nodular

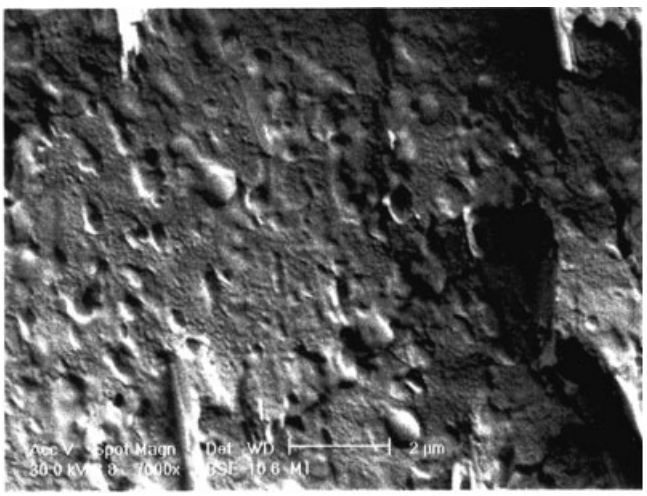

(a)

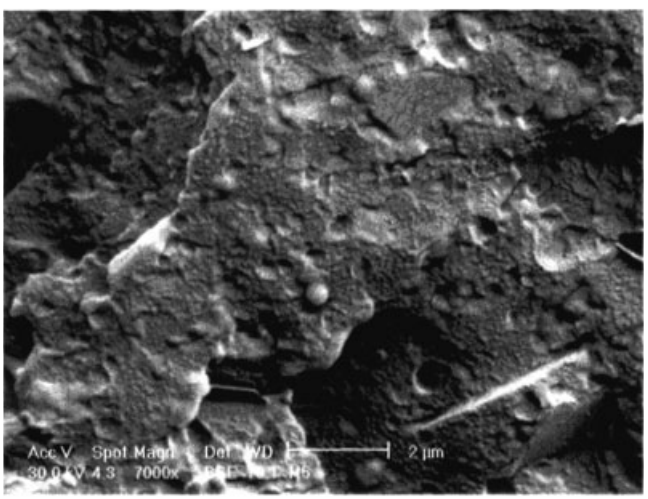

(b)

Figure 3 Morphologies of blends based on (PP/EPR)/EOC prepared with the twin-screw extruder. (a) (PP/EPR)/EOC (80)/20 and (b) (PP/EPR)/EOC/E-EA-MAH (80)/16/4.

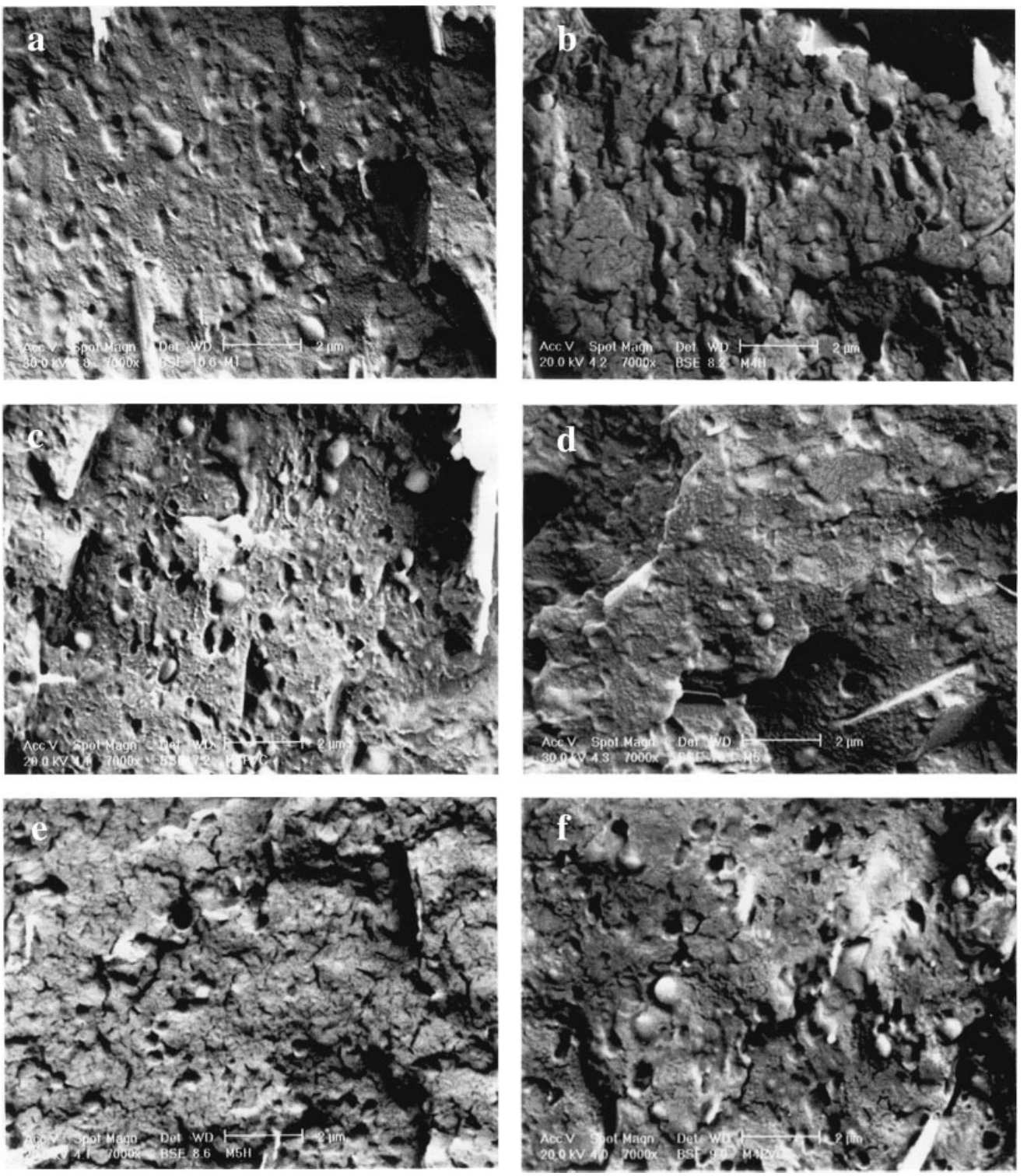

Figure 4 Morphologies of blends based on (PP/EPR)/EOC prepared with the twin-screw extruder. (a) (PP/EPR)/EOC (80)/20; (b) (PP/EPR)/EOC/oil (76)/19/5; (c) (PP/EPR)/EOC/PVC (76)/19/5; (d) (PP/EPR)/EOC/E-EA-MAH (76)/16/4; (e) (PP/EPR)/EOC/E-EA-MAH/oil (76)/15.2/3.8/5; (f) (PP/EPR)/EOC/E-EA-MAH/PVC (76)/15.2/3.8/5.

morphology; the presence of oil generates microcracks in the matrix phase and reduces the size of the dispersed particles (EPR and EOC phases) having a predominant spherical shape. Indeed, the plastification due to oil pollutant decreases considerably the viscosity of the blend in the melted environment.

The SEM analyses of (PP/EPR)/EOC/PVC (76)/19/5 blend [Fig. 4(c)] revealed two-phase morphology with a rather large polydispersity of ellipsoidal

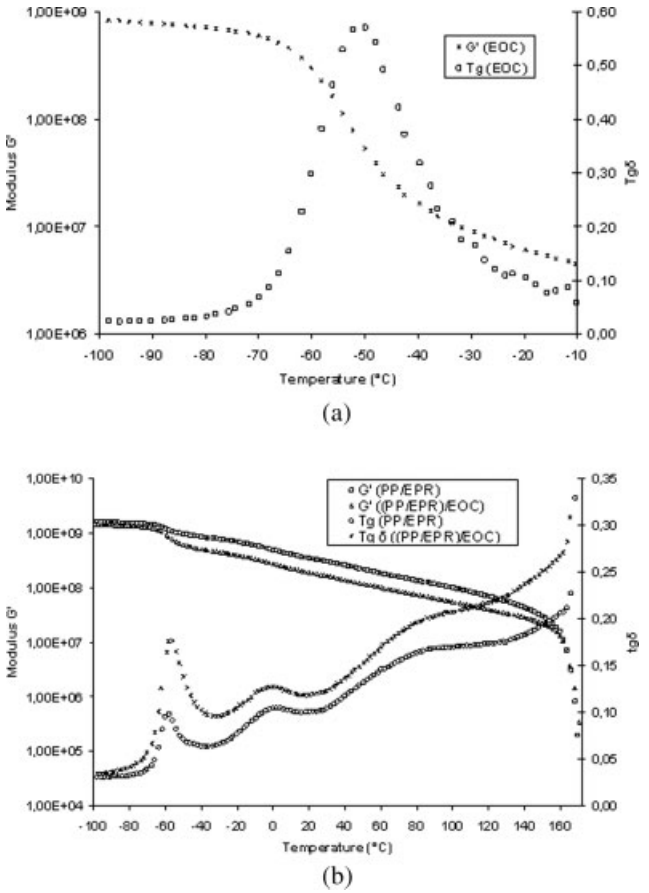

Figure 5 (a) Dynamic mechanical spectra of EOC. (b) Dynamic mechanical spectra of (PP/EPR) (78/22) and (PP/EPR)/EOC (80)/20.

PVC particles in the (PP/EPR)/EOC (80)/20 [Fig. 4(a)] matrix as well as the presence of cavities due to the extortion of nodules. This can be the result of high interfacial tension and coalescence.[13] The PVC domain size ranges from 0.2 to 0.3 μm in diameter.

In the case of the (PP/EPR)/EOC/E-EA-MAH/oil(76)/15.2/3.8/5 blend [Fig. 4(e)], the EOC particles possess a good adherence with the PP/EPR matrix in presence of the E-EA-MAH copolymer [Fig. 4(d)]. Indeed, the presence of the E-EA-MAH compatibilizer in the (PP/EPR)/EOC (80)/20 blends reduces the plastic effect of the pollutant on his morphology. But, in the case of the (PP/EPR)/EOC/E-EA-MAH/PVC (76)/15.2/3.8/5 blend [Fig. 4(f)], the adherence between the PVC and the (PP/EPR)/EOC blend is always weak even in the presence of the E-EA-MAH copolymer.

Viscoelastic behavior and thermal properties

(PP/EPR)/EOC (80)/20 blend

Figure 5(a,b) describes the viscoelastic response of the raw materials, EOC and (PP/EPR) 78/22, and of several blends. Three different relaxations are shown. One of them comes from the amorphous EPR component β_{EPR} (−58°C). The two other come from the semicrystalline parts and are named β_{PP} (1°C) and α_{PP} (94 °C) in order of increasing temperatures; α_{PP} results either from the shearing of the amorphous phase in the crystalline parts or from the movement of rotation of the chains around their longitudinal axis inside the crystal. In the case of the (PP/EPR)/EOC (80)/20 blend, two relaxation regions around −56 and 0°C are observed, which correspond to the glass transitions of the EPR elastomer and PP. Another relaxation region around 98°C is associated to the crystalline phase of the polypropylene (Table II).

The rheological properties of (PP/EPR) copolymer show that a combination of relaxation processes between those typical mechanisms from its components, PP and EPR, is exhibited. Consequently, four different relaxations are shown, two of them coming from the amorphous EPR component (being those at the lowest temperature and labeled γ_{EPR} and β_{EPR}) and the other two others, named β_{PP} and α_{PP}, stemming from the semicrystalline PP homopolymer. On the other hand, in EOC, only two well-defined, γ_{CEO} and β_{CEO}, processes are exhibited under tension. The relaxation traditionally observed at higher temperatures and called α relaxation in polyethylene homopolymer and some ethylene-α-olefin copolymers without very high comonomer content are practically not detected in EOC in either the tan δ or G' curves. The small shoulder appearing at the high side of temperatures in the β_{EOC} process seems to be due to a strong overlapping of the α_{EOC} process.[14] Because the oct-1-ene content is about 10% by mole in EOC, there is a subsequent reduction in the amount and perfection of crystallites where the α relaxation takes place and, consequently, the fusion peak of EOC is shifted to very low temperatures, and a nearly complete merging with the β_{EOC} occurs.[15] The nonco-

TABLE II
Rheological Characteristics of the Blends

Samples	$\beta_{EPR/EOC}$ (°C)	β_{PP} (°C)	α_{PP} (°C)
PP/EPR 78/22	$\beta_{EPR} = -58$	1	94
EOC	$\beta_{EOC} = -50$	–	–
(PP/EPR)/EOC (80)/20	−56	0	98
(PP/EPR)/EOC/oil (76)/19/5	−60	0	88
(PP/EPR)/EOC/PVC (76)/19/5	−57	0	$\beta_{PVC} = 86$
(PP/EPR)/EOC/E-EA-MAH (80)/16/4	−56	0	98
(PP/EPR)/EOC/E-EA-MAH/oil (76)/15.2/3.8/5	−60	−4	94
(PP/EPR)/EOC/E-EA-MAH/PVC (76)/15.2/3.8/5	−56	0	$\beta_{PVC} = 85$

crystallization of PP and EOC in the same type of crystal lattice gives rise to two different crystalline phases, and, on the other hand, the immiscibility of the distinct amorphous chains provokes the existence of three differentiated amorphous phases stemming from the corresponding ones in the semicrystalline PP, the totally amorphous EPR, and the semicrystalline EOC. Moreover, Figure 5(b) also shows a clear dependence of the storage modulus with the blend composition, being more significant from −56°C to increasing temperatures, that is, above the EOC glass transition.[16–22] The incorporation of the plastomer EOC decreases significantly the rigidity in the blends. The different relaxation processes observed are analyzed separately in the order of increasing temperatures.

Effect of the compatibilizer in the (PP/EPR)/EOC (80)/20 blend

The storage modulus and the loss tangent as a function of temperature for (PP/EPR)/EOC and (PP/EPR)/EOC/E-EA-MAH (80)/16/4 blends are displayed in Figure 6; the compatibilizer E-EA-MAH leads to a modification of the relaxations associated to the glass transitions, or it is localized at the interface between the (PP/EPR) and EOC phases as mentioned in the morphological study. The E-EA-MAH copolymer induces a better adherence and cohesion of the whole material.

Figure 7 shows the DSC heating curves only for (PP/EPR), EOC, (PP/EPR)/EOC, and (PP/EPR)/EOC/E-EA-MAH blends over the temperature range −100–200°C and Table III lists the DSC characteristics of both virgin polymers and their blends. (PP/EPR) displayed two peaks: a sharp endothermic melting process of polypropylene 167°C (T_{mPP}) and a second peak of weak intensity associated to the sequences ethylene in EPR at 117°C (T_{mE}). The EOC curve shows a peak that appears at about 40°C (T_{mEOC}), indicating the presence of a crystalline region, and a glass transition at about −50°C. The melting temperature (T_m) and heat of fusion (ΔH_{PP}) were determined from the heating cycle of DSC scans.

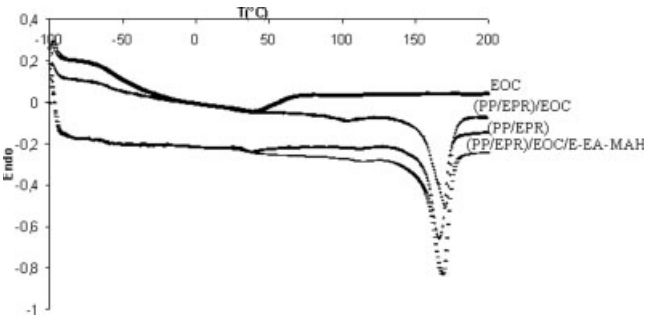

Figure 7 DSC of (PP/EPR), EOC, (PP/EPR)/EOC, and (PP/EPR)/EOC/E-EA-MAH.

The blends show a broad melting endotherm, which is probably related to changes in the distribution of (PP/EPR) crystal size when elastomers are added. The thermal behavior during the first melting for (PP/EPR)/EOC seems to point to immiscibility in the blends owing to the constancy of the melting temperatures of the two components, as listed in Table III and displayed in Figure 7. A melting peak was detected in the EOC melting curve at 40°C, indicating a certain degree of crystallinity. As should be expected, the results show that as the EOC content increases, the crystallinity degrees and the heat of fusion decreases in relation to pure (PP/EPR). On the other hand, the presence of the EOC copolymer in the blend generates a displacement of the T_{mEOC} peak towards the low temperatures induced by the interactions between the sequences ethylene of the (PP/EPR) and EOC phases.

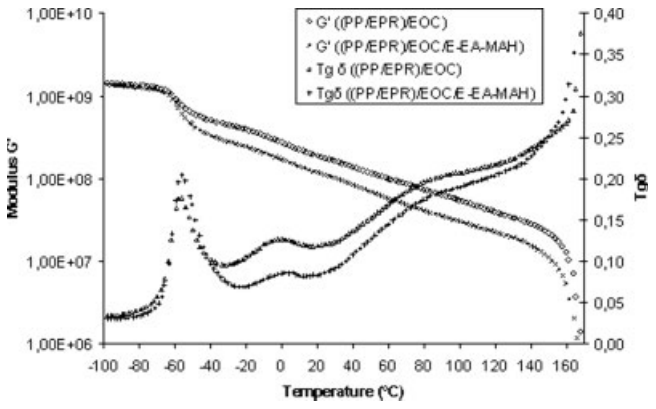

Figure 6 Dynamic mechanical spectra of (PP/EPR)/EOC (80)/20 and (PP/EPR)/EOC/E-EA-MAH (80)/16/4.

TABLE III
Thermal Characteristics of the Blends

Samples	T_{mEOC} (°C)	T_{mE} (°C)	T_{mPP} (°C)	ΔH_{PP} (J/g)
(PP/EPR) 78/22	–	117	167	−52.5
EOC	40	–	–	–
(PP/EPR)/EOC (80)/20	40	113	166	−41.5
(PP/EPR)/EOC/oil (76)/19/5	42	113	168	−40
(PP/EPR)/EOC/PVC (76)/19/5	40	113	166	−41
(PP/EPR)/EOC/E-EA-MAH (80)/16/4	40	105	170	−44
(PP/EPR)/EOC/E-EA-MAH/oil (76)/15.2/3.8/5	40	105	170	−39
(PP/EPR)/EOC/E-EA-MAH/PVC (76)/15.2/3.8/5	40	105	170	−43.5

As for the (PP/EPR)/EOC/E-EA-MAH blend compatibilized with the E-EA-MAH copolymer, a reduction of the melting temperature of the ethylene sequences of the EPR (T_{mE}) was observed. The E-EA-MAH copolymer that is localized at the interface between EOC and (PP/EPR) phases, according to the morphological observations and viscoelastic behavior, is at the origin of this variation. On the other hand, the presence of the E-EA-MAH copolymer in the (PP/EPR)/EOC blend generates a reduction of the melting temperature T_{mP} and of the heat of fusion (H_{PP}); it is probably due to a variation of the percentage of crystallinity and/or of the thickness of the crystalline lamellae in presence of the E-EA-MAH.

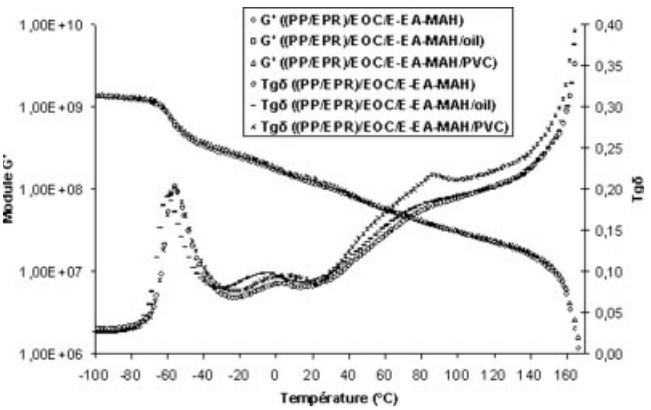

Figure 9 Dynamic mechanical spectra of (PP/EPR)/EOC/E-EA-MAH, (PP/EPR)/EOC/E-EA-MAH/oil, and (PP/EPR)/EOC/E-EA-MAH/PVC.

Effect of pollutants in the (PP/EPR)/EOC (80)/20 blend

Figure 8 shows dynamic mechanical spectra for the (PP/EPR)/EOC (80)/20, (PP/EPR)/EOC/oil (76)/19/5, and (PP/EPR)/EOC/PVC (76)/19/5 blends; the presence of the oil in the (PP/EPR)/EOC blend generated a considerable reduction of the complex dynamic modulus (G') that is due to the plasticizing effect of oil. This effect concerned the components of the (PP/EPR)/EOC/oil (76)/19/5 blend. Indeed, a displacement of the peaks of $\beta_{EPR/EOC}$ and $\alpha_{(PP/EPR)}$ relaxation towards the low temperatures, respectively, with ΔT of 4°C and 10°C is observed.

The presence of PVC pollutant generates the apparition of a new relaxation near 86°C associated to the glass transition of this polymer. Thus, the PVC does not present any miscibility with the other components of the (PP/EPR)/EOC/PVC (76)/19/5 blend. The displacement of the relaxation $\beta_{EPR/EOC}$ is attributed to a supplementary thermomechanical treatment for the introduction of PVC that generate a variation of the length of the chains. On the other hand, the peak of PVC is broadened in the presence of E-EA-MAH, which can be attributed to the physical interactions between the pollutant and the compatibilizer.

The reduction of the modulus G' in presence of the oil for engine (Fig. 9) in the (PP/EPR)/EOC/oil blend is limited in presence of the compatibilizer E-EA-MAH ((PP/EPR)/EOC/E-EA-MAH/oil); it is due to the interactions between the pollutant and the copolymer E-EA-MAH (high polarity of the two constituents).

Thermal properties of (PP/EPR)/EOC/oil and (PP/EPR)/EOC/PVC blends (Fig. 10 and Table III) in the presence and in the absence of compatibilizer polluted, respectively, with oil and PVC are summarized in Table III. The presence of oil induces a displacement of the melting temperatures of EOC (T_{mEOC}) and of propylene sequences of the (PP/EPR) (T_{mPP}) towards the high temperatures ($\Delta T = 2$°C) with the reduction of the value of the heat of fusion (ΔH_{PP}) of the polypropylene phase. These results can be

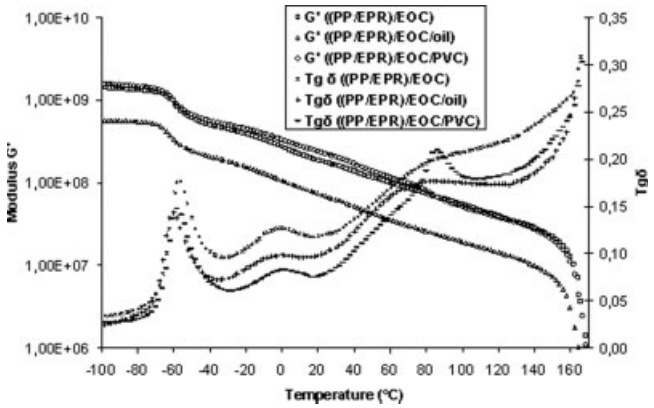

Figure 8 Dynamic mechanical spectra of (PP/EPR)/EOC, (PP/EPR)/EOC/oil, and (PP/EPR)/EOC/PVC.

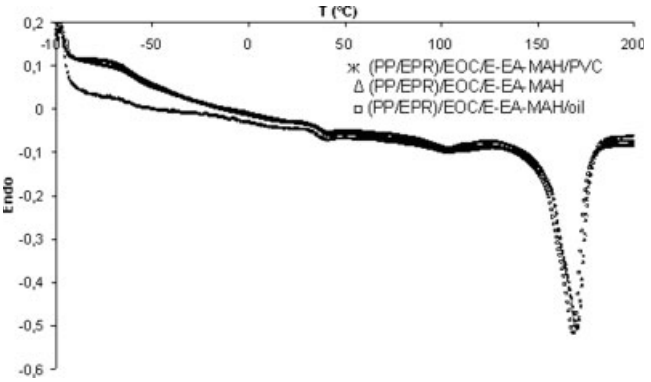

Figure 10 DSC of (PP/EPR)/EOC/E-EA-MAH, (PP/EPR)/EOC/E-EA-MAH/oil, and (PP/EPR)/EOC/E-EA-MAH/PVC.

explained by a reduction of the rate of crystallinity and by the increase of the size of the crystals. The plasticizing effect of oil generates the flexibility of the chains in the blends and facilitates the formation of crystals while increasing their sizes. In the case of the compatibilized blend, the presence of E-EA-MAH copolymer attenuates the plasticizing effect of the oil for engine in agreement with the morphological and thermomechanical dynamic results.

Concerning the (PP/EPR)/EOC/PVC and (PP/EPR)/EOC/E-EA-MAH/PVC blend (Fig. 10), the PVC does neither induce any variation of the temperature of the different peaks of fusion (T_{mEOC}, T_{mPP}, and T_{mE}) nor of the value of the heat of fusion (ΔH_{PP}) of the crystalline phase. It means, by analogy with the morphological observations and the viscoelastic properties, that the PVC does not present any miscibility with the other components of the blends.

CONCLUSIONS

Morphological, viscoelastic, and thermal results showed that (PP/EPR) copolymer blended with EOC copolymer are not miscible. The presence of the E-EA-MAH copolymer that does not present interaction with the PVC pollutant improves considerably the adherence to the interface between the (PP/EPR) and EOC phases and attenuates the plasticizing effect of the oil for engine (constant value of the modulus G' in presence of the oil for engine and the E-EA-MAH copolymer).

The incorporation of oil in the blends generates microcracks in the (PP/EPR) phase, whereas PVC forms nonmiscible spherical particles in the blends. In presence of oil, there is a shift of the relaxation peak associated to the glass transition of the EOC and EPR phases. There is also a shift of the melting peaks of propylene sequences and of the EOC phase.

References

1. Block, D. G. Plast World 1995, 37.
2. Woo, L.; Ling, M. T. K.; Westphal, S. P. Antec 1995, 3, 2284.
3. Manders, P. W.; Mod Plast November 1993, 45.
4. Murphy, J. High Perform Plast 1994, 2.
5. Kallel, T.; Massardier-Nageotte, V.; Jaziri, M.; Gérard, J. F.; Elleuch, B. Plast Recycl Technol 2003, 19, 61.
6. Tomasetti, E.; Legras, R.; Henri-Mazeaud, B.; Nysten, B. Polymer 2000, 41, 6597.
7. Radonjic, G.; Gubeljak, N. Macromol Mater Eng 2002, 287, 122.
8. Pires, M.; Mauler, R. S.; Liberman, S. A. J Appl Polym Sci 2004, 92, 2155.
9. Seki, M.; Yamauchi, S.; Matsushita, Y. J Phys Chem Solid 1999, 60, 1333.
10. Hlavata, D. Macromol Symp 2001, 176, 93.
11. Thamm, R. C. Rubber Chem Technol 1976, 50, 24.
12. D'Orazio, L.; Mancarella, C.; Martuscelli, E. Polymer 1991, 32, 1186.
13. Ajji, A.; Utracki, L. A. Polym Eng Sci 1996, 36, 1574.
14. Arranz-Andrés, J.; Benavente, R.; Pena, B.; Pérez, E.; Cerrada, M. L. J Polym Sci Part B: Polym Phys 2002, 40, 1869.
15. Cerrada, M. L.; Benavente, R.; Pérez, E. J Mater Res 2001, 16, 1103.
16. Cerrada, M. L.; Benavente, R.; Pérez, E.; Moniz-Santos, J.; Ribeiro, M. R. Polymer 2001, 42, 7197.
17. Van den Eynde, S.; Mathot, V. B. F.; Koch, M. H. J. Reynaers, H. Polymer 2000, 41, 4889.
18. Prieto, O.; Pereña, J. M.; Benavente, R.; Pérez, E.; Cerrada, M. L. Polymer, submitted.
19. Lorenzo, V.; Pereña, J. M.; Fatou, J. M. G. Makromol Chem 1989, 172, 25.
20. Benavente, R.; Pérez, E.; Quijada, R. J Polym Sci Part B: Polym Phys 2001, 39, 277.
21. Cerrada, M. L.; de la Fuente, J. L.; Fernández-García, M.; Madruga, E. L Polymer 2001, 42, 4647.
22. Cerrada, M. L.; Benavente, R.; Pérez, E. Macromol Chem Phys 2002, 203, 718.